# Comparison of Field Oriented Control and Direct Torque Control

Mirza Abdul Waris Begh*[1], and Hans-Georg Herzog*[2]
*Technical University of Munich, Germany
e-mail: [1]mirza.begh@tum.de, [2]hg.herzog@tum.de

***Abstract*—Field oriented control (FOC) and Direct torque control (DTC) are the two most popular vector control methods for electric motor drives. FOC uses linear controllers and pulse width modulation (PWM) to control the fundamental components of the load voltage. On the other hand, DTC is a nonlinear strategy that directly generates the voltage vectors in the absence of a modulator. This paper presents a comparative study between the two control schemes. The pros and cons of both the methods are separately discussed for two candidate machines: Induction Machine (IM) and Permanent Magnet Synchronous Machine (PMSM). The comparison is based on various criteria including basic control characteristics, dynamic performance, parameter sensitivity, and implementation complexity. The discussion is supported with results from various articles, and a criterion to draw a fair comparison between the performance of the two schemes is also presented.**

**Keywords—***Field Oriented Control (FOC), Direct Torque Control (DTC), Induction Machine (IM), Permanent Magnet Synchronous Machine (PMSM).*

## I. Introduction

FOR more than a century, electric motors have been an integral part of our lives. Without them, there would have been no Industrial Revolution, and our lifestyle would be quite different from what we have come to enjoy and expect. Motors are often unknown and unseen, quietly doing many of the mundane chores that we take for granted, but they are an important element of the system [1].

First electric drives were completely DC based, since the DC motor was for a long time the only type of motor capable of high dynamic performance. Regardless of its certain drawbacks – namely a complex construction (especially with a fully compensated machine), lower efficiency compared to AC machines, and high cost – the torque control of the DC motor has nevertheless always been very straightforward, as the air-gap flux and the torque can be controlled separately. However, it requires regular maintenance due to its carbon brushes [2].

Over the past few decades, Induction Motors (IMs) have become the true workhorses for industrial applications due to their distinct advantages including simple construction, reliability, robustness, and less maintenance [3], [4]. However, in recent years, Permanent Magnet Synchronous Motors (PMSMs) gained significance over IMs due to their superior efficiency, greater power density and larger high torque to inertia ratio [5]–[7]. This prominent shift of the industrial drives from DC to AC drives paved the way for search of better and reliable control techniques. Additionally, the main driver behind the advent of advanced control techniques for AC machines was the decoupled control of torque and flux in a DC machine. The dynamic performance for both IM and PMSM drives depends upon the effective control of electromagnetic torque ($T_e$) and magnetic flux ($\Phi$) [8].

### A. Background

The first speed-controlled AC drives with sinusoidal excitation were Synchronous Machines (SMs), since early inverter topologies based on mercury-arc switches were not capable of handling reactive power. A milestone in the field of speed control of AC machines was the invention of the cycloconverter capable of reactive power handling in the early 1930s. This also enabled the use of induction machines in the speed control, although the dynamic performance and the stability of the machines were very poor. Induction machines were more robust and cheaper, and unlike the synchronous machines they did not have the problem of losing synchronism. The introduction of the space vector theory for multi-phase AC machines in 1959 [9], and the theory of pulse width modulation (PWM) for AC drives in 1964 [10] finally made it possible for AC motors to be used in speed controlled drives. This was also due to the introduction of the silicon power switches in the 1950s, which made it possible to switch higher currents and voltages at faster speeds [2].

Traditionally scalar control was employed to control flux and torque by varying the voltage and applied frequency. It is a simple and economic method that controls the voltage magnitude in proportion to change in the frequency. The idea is to maintain a constant magnetising current effectively keeping the air-gap flux constant [3]. However this method is characterised by very poor transient (dynamic) performance and hence is effective in steady state only [3], [4], [11], [12].

Since the speed of an IM is close to synchronous speed, a better method of speed control is to change the stator frequency. Consequently the operating slip will be small and the slip power loss in the rotor circuit will also be small [13]. However, this would require a frequency converter, which is expensive. In essence flux regulation schemes such as Volt/Hertz and current slip frequency control were extensively used in the industry [14] and provided satisfactory steady state performance, however the dynamic performance still lagged DC drives until the early 1970s.

In 1968 the concept of *Indirect Field Oriented Control* (IFOC) was put forth by Hasse [15], [16]. Later in 1971 *Direct Field Oriented Control* (DFOC) was developed within Siemens

by Blaschke [17]. Both authors proposed an orientation aligned with the rotor flux vector. In terms of the adoption by the industry, Toshiba was the first to implement a vector controlled AC drive (1979), which consisted of an inverter and an induction motor. In 1980 Werner Leonhard at the Technische Universität Braunschweig further developed FOC techniques opening up more opportunities for AC drives.

In FOC the motor equations are transformed (rewritten) in a coordinate system that rotates in synchronism with rotor flux vector. In field coordinate system - under constant rotor flux amplitude there is a linear relationship between control variables and torque. This transformation has a good physical basis, as it corresponds to the decoupled torque production in a separately excited DC motor. However from the theoretical point of view, the concept of field orientation is not restricted to rotor flux orientation but also possible with stator or air-gap flux [18]. In the late 1980s there were few publications on stator flux orientation [19] that presented some advantages over the rotor flux-oriented control. A generalization is the concept of universal field orientation [20].

When in the mid 1980s, it appeared that the control systems would be standardized on the basis of the FOC philosophy, there appeared the innovative studies of Depenbrock [21], [22] and Takahashi and Noguchi [23], which depart from the idea of coordinate transformation and the analogy with DC motor control. Depenbrock in 1986 (within Brown Boveri, now ABB) proposed *Direct Self-Control* (Direkte Selbstregelung), intended mainly for high-power drives with voltage source inverters. Whereas Takahashi and Noguchi (1986) proposed *Direct Torque Control*, mainly intended for low and medium voltage drives. These innovators proposed to replace motor decoupling with *bang-bang* self-control, which goes together very well with on-off operation of inverter semiconductor power devices. This control strategy is commonly referred as *Direct Torque Control* (DTC). Uwe Baader carried out a deeper study of the DTC concept and made significant contributions [24].

Unlike FOC with stator current as inner control objective, Direct Self-Control (DSC) and DTC govern the stator flux by means of hysteresis controls. DSC was developed for high power and traction application. Both possess high torque dynamics compared to FOC. However, both the control techniques have inherent drawbacks of variable switching frequency and higher torque ripple. Since then it has been continuously worked by researchers to overcome these inherent drawbacks. These problems opened various opportunities for researchers to work on different kinds of strategies to avoid the variable switching frequency [25]–[27], but sticking to the fundamental concept of torque control.

### B. Organisation of the paper

The paper is organised as follows: In Section 2, the model of an AC machine is derived based on the fundamental wave model. The two control schemes for an Induction machine are presented in Section 3, which is divided into two major parts containing a detailed description of Field oriented control in Section 3.1 and Direct torque control in Section 3.2. Section 4 presents a comparison of the two control schemes for various scenarios with conclusions towards the end. In Section 5 a brief discussion about the control methods of PMSM is presented with some conclusions and Section 7 concludes the paper.

## II. Modelling of the AC Machine

### A. Structure of the AC machine

An AC machine mainly consists of stator and rotor windings. The simplified structure of an AC machine is depicted in Fig. 1. The stator consists of the phases A, B, C whereas the rotor holds the phases U, V, W. The following relations apply for the machines [28]:

- Stator and rotor are built symmetrically.
- The phases of stator and rotor are wound symmetrically. They are displaced by 2/3 of the *pole pitch* $\tau_p$, that means by 2/3 of half of the spatial period of the magnetomotive force fundamental wave. The stator phases have $N_s$ windings respectively the rotor phases have $N_r$ windings.
- Both winding sets are connected to a star-point which is floating.

To determine the rotor position, the mechanical angle $\theta_m$ is defined (see Fig. 1). The electrical angle $\theta_e$ as well as its time derivative, the electrical speed $\omega_e$, are related to the mechanical angle, respectively the rotor speed by the pole pair number *p*.

$$\theta_e = p \cdot \theta_m \tag{1a}$$

$$\omega_e = p \cdot \omega_m \tag{1b}$$

For simplicity reasons but without loss of generality the number of pole pairs *p* is assumed to be 1. Hence the coils are displayed by $120^\circ$ and the mechanical angle is equal to the electrical angle. When 3-phase balanced voltages are supplied to the stator windings, a rotating magnetic field with constant magnitude is created which rotates inside the air-gap with speed $\omega_e$. This flux is mainly responsible for generation of torque to enable machine operation.

### B. Assumptions for the Fundamental Wave Model

Similar to the DC machine the electromagnetic, mechanical and thermal processes inside the AC machine are in general complex and non-linear. For this reason following assumptions are made for the model [28]:

- The spatial distribution of the magneto-motive force and the magnetic field in the air-gap are assumed to be sinusoidal. Therefrom results the name fundamental wave model. In reality there are harmonic waves of higher orders. Even though some measures (choice of slot number and distribution of windings) are taken to reduce them, they are caused by the discrete position of the stator/rotor slots and windings and hence can't be suppressed completely.
- The magnetic flux has no axial component. We consider only the cross-sectional area (2D).

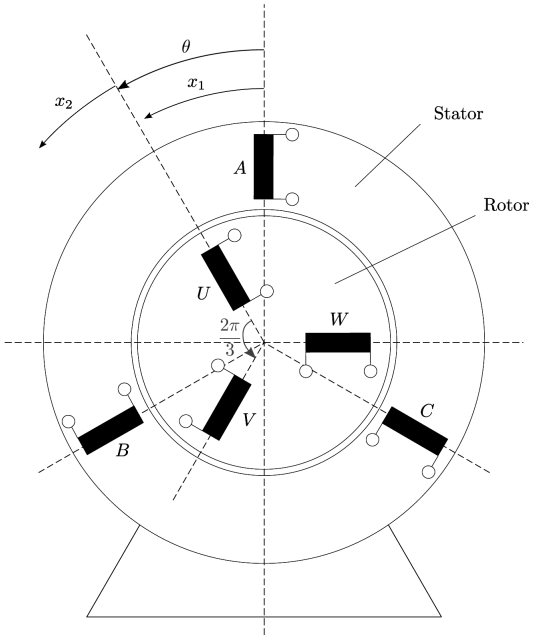


Fig. 1: Principle structure of an AC Machine, $x_1$: Coordinates w.r.t the Stator; $x_2$: Coordinates w.r.t the Rotor; $\theta$: Angle between the axes of the phases A and U. [28]

- The magnetic material exhibits linear properties. The effects of magnetic saturation and hysteresis are neglected.
- Only ohmic losses are considered. Iron and Eddy current losses are neglected.
- The influence of temperature on resistance and inductance are neglected.
- All coils of the machine have identical properties i.e. they are symmetrical.

### C. Electrical Differential Equations

Like a DC machine, the electrical equivalent circuit for an AC machine can be drawn as shown in Fig. 2. The general electrical differential equation for the AC machine is written as:

$$u_k = R_l \cdot i_k + \frac{d\Psi_k}{dt} \tag{2}$$

where the index $k$ stands for the phases ($k \in$\{A, B, C, U, V, W\}). The rotor and stator are distinguished by the index ($l \in s, r$).

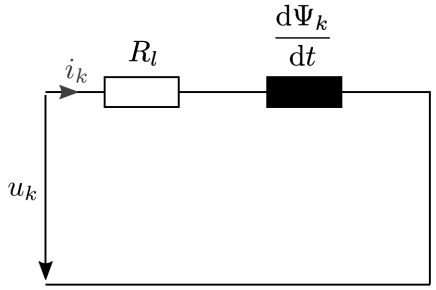


Fig. 2: Equivalent circuit of AC machine [28].

Hence for the stator phases following equations for the stator voltage $u_k$, described by the current $i_k$ and the flux linkage $\Psi_k$ with the index ($k \in$\{A, B, C\}) and the resistor $R_s$ hold true:

$$u_A = R_s \cdot i_A + \frac{d\Psi_A}{dt} \tag{3a}$$

$$u_B = R_s \cdot i_B + \frac{d\Psi_B}{dt} \tag{3b}$$

$$u_C = R_s \cdot i_C + \frac{d\Psi_C}{dt} \tag{3c}$$

The equations for the rotor phases are described analogously by the index ($k \in$\{U, V, W\}) and the resistor $R_r$ :

$$u_U = R_r \cdot i_U + \frac{d\Psi_U}{dt} \tag{4a}$$

$$u_V = R_r \cdot i_V + \frac{d\Psi_V}{dt} \tag{4b}$$

$$u_W = R_r \cdot i_W + \frac{d\Psi_W}{dt} \tag{4c}$$

The per phase quantities, described above, can be written in vector notation as follows:

$$\underline{u}_s = [u_A, u_B, u_C]^T \qquad \underline{u}_r = [u_U, u_V, u_W]^T \tag{5}$$

$$\underline{i}_s = [i_A, i_B, i_C]^T \qquad \underline{i}_r = [i_U, i_V, i_W]^T \tag{6}$$

$$\underline{\Psi}_s = [\Psi_A, \Psi_B, \Psi_C]^T \qquad \underline{\Psi}_r = [\Psi_U, \Psi_V, \Psi_W]^T \tag{7}$$

Then the basic voltage differential equations (3) and (4) can be simplified to:

$$\underline{u}_s = R_s \cdot \underline{i}_s + \frac{d\underline{\Psi}_s}{dt} \tag{8}$$

$$\underline{u}_r = R_r \cdot \underline{i}_r + \frac{d\underline{\Psi}_r}{dt} \tag{9}$$

### D. Space Vectors and Transforms

The AC machines are ideally fed by sinusoidal voltages. Since the construction of the machines is such that the phases are distributed in space, the electrical quantities like current are thus distributed in time and space. Hence it is quite easy to represent the electrical quantities using space vectors [28]. However due to its construction the general frame of reference, also known as *abc* reference frame, depicted in Fig. 3, describes all the electrical quantities along the three axes. In order to simplify the calculations and reduce the number of the manipulated variables two famous transforms are generally employed.

*1)* ***The Clarke Transformation****:* The mathematical conversion of the three phase voltages $u_A, u_B$ and $u_C$ to $\underline{u}_s$ is known as the *Clarke Transformation*. The space vector $\underline{u}_s$ can be described in the Cartesian $\alpha - \beta$ coordinate system as introduced in Fig. 3, since three linear dependent quantities can be expressed by two linear independent variables. Hence the $\alpha$ and $\beta$ components can be summarized as a complex number:

$$\begin{aligned} \underline{u}_s &= \frac{2}{3}(u_A + u_B e^{j.120^\circ} + u_C e^{j.240^\circ}) \\ &= \frac{2}{3}\left[u_A - \frac{1}{2}u_B - \frac{1}{2}u_C + j\left(\frac{\sqrt{3}}{2}u_B - \frac{\sqrt{3}}{2}u_C\right)\right] \end{aligned} \tag{10}$$

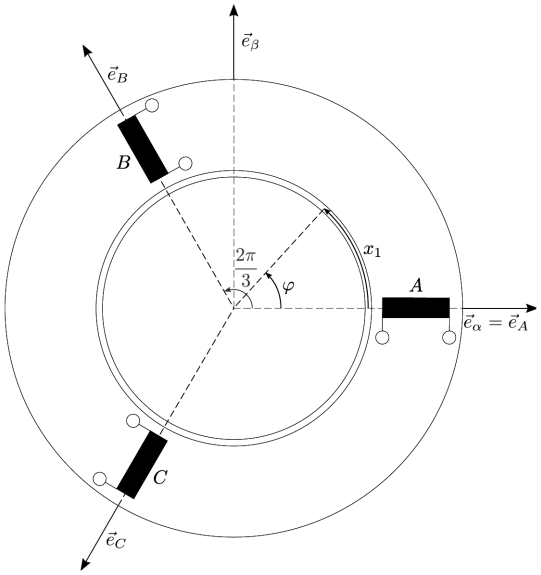


Fig. 3: Schematic Representation of the Stator Winding in the *abc* frame [28].

The transformation from phase values to space vector can also be expressed in the matrix notation:

$$\begin{bmatrix} u_\alpha \\ u_\beta \end{bmatrix} = \frac{2}{3} \begin{bmatrix} 1 & -\frac{1}{2} & -\frac{1}{2} \\ 0 & \frac{\sqrt{3}}{2} & -\frac{\sqrt{3}}{2} \end{bmatrix} \begin{bmatrix} u_A \\ u_B \\ u_C \end{bmatrix} \tag{11}$$

Here the factor $\frac{2}{3}$ is applied, to scale the length of the space vector to the amplitude of the phase values.

*2)* ***The Park Transformation****:* The previous section discussed a coordinate system fixed to the stator $(\vec{e}_\alpha; \vec{e}_\beta)$. If any space vector is rotated by an arbitrary angle $\varphi_K$, it can be represented in a different coordinate system. For example a coordinate system fixed to the rotor $(\vec{e}_k; \vec{e}_l)$ or the flux $(\vec{e}_d; \vec{e}_q)$. Such a rotation around the origin can be described by the rotation matrix:

$$\mathcal{T}_\mathcal{P}(\varphi_K) = \begin{bmatrix} \cos(\varphi_K) & -\sin(\varphi_K) \\ \sin(\varphi_K) & \cos(\varphi_K) \end{bmatrix} \tag{12}$$

For electrical drive systems the transformation is famous as *Park Transformation* [30]. Fig. 4 illustrates the definition of the angle $\varphi_K$. Table 1 presents an overview of the different coordinate systems relevant for our application.

Table I: Useful Frames of Reference.

| Frame | Abbrev. | Angle | Notation | Transform |
|---|---|---|---|---|
| Stator | $(a, b, c)$ | - | $\underline{u}_x^{abc}$ | - |
| Stationary | $(\alpha, \beta)$ | - | $\underline{u}_x^{\alpha\beta}$ | Clarke |
| Rotor Flux | (d,q) | $\varphi_K$ | $\underline{u}_x^{dq}$ | Clarke & Park |

### *E. Electromagnetic Relations*

Flux plays a vital role in the operation of AC machines and we shall assume that all the coils are linked by flux $\underline{\Phi}$. The magnetic flux $\underline{\Phi}$ of a coil can be decomposed into two

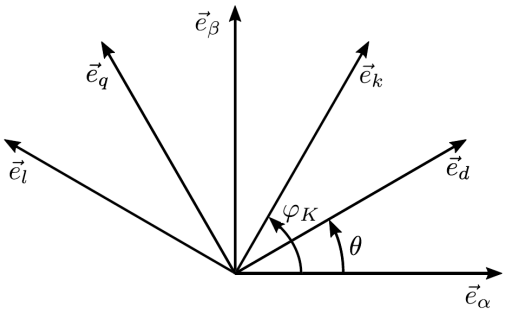


Fig. 4: Definition of new coordinate system rotated by angle $\varphi_K$ using Park transform [28].

components, namely, the leakage flux $\underline{\Phi}_\sigma$ and the main flux $\underline{\Phi}_h$. The flux lines that do not cross the air-gap and are only linked to their respective windings constitute the leakage flux $\underline{\Phi}_\sigma$, while the flux lines that cross the air-gap and link the two windings, i.e. stator and rotor windings, constitute the main flux $\underline{\Phi}_h$. Thus the main flux is responsible for the operational behaviour of the AC machines and contributes to the resulting torque [28]. So:

$$\underline{\Phi} = \underline{\Phi}_h + \underline{\Phi}_\sigma \tag{13}$$

According to Hopkins law, the product of the reluctance and flux gives the magnetomotive force $\underline{\Theta}$, which can be written as:

$$\underline{\Theta} = N \cdot \underline{i} = R_m \cdot \underline{\Phi} \tag{14}$$

$$\Rightarrow \underline{\Phi} = \frac{\underline{\Theta}}{R_m} = \frac{N \cdot \underline{i}}{R_m} \tag{15}$$

where $N$ is the number of the windings, $i$ is the current flowing through the winding and $R_m$ is the reluctance. With the equivalent decomposition of $R_m = R_{mh} + R_{m\sigma}$ the main fluxes can be written in the stator $\Phi^s_{hs}$ and the rotor $\Phi^r_{hr}$ coordinates:

$$\underline{\Phi}^s_{\sigma s} = \frac{\underline{\Theta}^s_s}{R_{m\sigma s}} = \frac{N_s \cdot \underline{i}^s_s}{R_{m\sigma s}} \tag{16}$$

$$\underline{\Phi}^r_{\sigma r} = \frac{\underline{\Theta}^r_r}{R_{m\sigma r}} = \frac{N_r \cdot \underline{i}^r_r}{R_{m\sigma r}} \tag{17}$$

$$\underline{\Phi}^s_h = \frac{\underline{\Theta}^s_h}{R_{mh}} = \frac{\underline{\Theta}^s_s + \underline{\Theta}^s_r}{R_{mh}} = \frac{N_s \cdot \underline{i}^s_s + N_r \cdot \underline{i}^s_r}{R_{mh}} \tag{18}$$

$$\underline{\Phi}^r_h = \frac{\underline{\Theta}^r_h}{R_{mh}} = \frac{\underline{\Theta}^r_s + \underline{\Theta}^r_r}{R_{mh}} = \frac{N_r \cdot \underline{i}^r_s + N_r \cdot \underline{i}^r_r}{R_{mh}} \tag{19}$$

The flux linkage $\Psi$ is defined as the product of the magnetic flux multiplied with the number of windings $N$:

$$\underline{\Psi} = N \cdot \underline{\Phi} = N \cdot \frac{\underline{\Theta}}{R_m} = N \cdot \frac{N \cdot \underline{i}}{R_m} = \frac{N^2 \cdot \underline{i}}{R_m} \tag{20}$$

By taking the derivate with the respect to the current $\underline{i}$ the general definition of *inductance L* is derived:

$$L = \frac{\underline{\Psi}}{\underline{i}} = \frac{N^2}{R_m} \tag{21}$$

Hence the leakage flux linkages can be rewritten as:

$$\begin{aligned}\text{Stator}: \underline{\Psi}^s_{\sigma s} &= N_s \cdot \underline{\Phi}^s_{\sigma s} = N_s \cdot \frac{\underline{\Theta}^s_s}{R_{m\sigma s}} \\ &= N_s \cdot \frac{N_s \cdot \underline{i}^s_s}{R_{m\sigma s}} = \frac{N_s^2 \cdot \underline{i}^s_s}{R_{m\sigma s}}\end{aligned} \tag{22}$$

$$\begin{aligned}\text{Rotor}: \underline{\Psi}^r_{\sigma r} &= N_r \cdot \underline{\Phi}^r_{\sigma r} = N_r \cdot \frac{\underline{\Theta}^r_r}{R_{m\sigma r}} \\ &= N_r \cdot \frac{N_r \cdot \underline{i}^r_r}{R_{m\sigma r}} = \frac{N_r^2 \cdot \underline{i}^r_r}{R_{m\sigma r}}\end{aligned} \tag{23}$$

The corresponding inductances for the leakage flux linkages are defined as:

$$\text{Stator}: L_{\sigma s} = \frac{d\underline{\Psi}^s_s}{d\underline{i}^s_s} = \frac{N_s^2}{R_{m\sigma s}} \tag{24}$$

$$\text{Rotor}: L_{\sigma r} = \frac{d\underline{\Psi}^r_r}{d\underline{i}^r_r} = \frac{N_r^2}{R_{m\sigma r}} \tag{25}$$

Analogously the main flux linkage and the respective inductances are defined as:

$$\begin{aligned}\text{Stator}: \underline{\Psi}^s_{hs} &= N_s \cdot \underline{\Phi}^s_h = N_s \cdot \frac{\underline{\Theta}^s_s}{R_{mhs}} \\ &= N_s \cdot \frac{\underline{\Theta}^s_s + \underline{\Theta}^s_r}{R_{mh}} = N_s \cdot \frac{N_s \cdot \underline{i}^s_s + N_r \cdot \underline{i}^s_r}{R_{mh}}\end{aligned} \tag{26}$$

$$\begin{aligned}\text{Rotor}: \underline{\Psi}^r_{hr} &= N_r \cdot \underline{\Phi}^r_h = N_r \cdot \frac{\underline{\Theta}^r_r}{R_{mhr}} \\ &= N_r \cdot \frac{\underline{\Theta}^r_s + \underline{\Theta}^r_r}{R_{mh}} = N_r \cdot \frac{N_r \cdot \underline{i}^r_s + N_r \cdot \underline{i}^r_r}{R_{mh}}\end{aligned} \tag{27}$$

$$\text{Stator}: L_{hs} = \frac{d\underline{\Psi}^s_{hs}}{d\underline{i}^s_s} = \frac{N_s^2}{R_{mh}} \tag{28}$$

$$\text{Rotor}: L_{hr} = \frac{d\underline{\Psi}^r_{hr}}{d\underline{i}^r_r} = \frac{N_r^2}{R_{mh}} \tag{29}$$

Mutual inductance $L_m$, which represents the connection between stator and rotor across the air-gap, is defined as:

$$\text{Stator to Rotor}: L_{sr} = \frac{d\underline{\Psi}^s_{hs}}{d\underline{i}^s_r} = \frac{N_s \cdot N_r}{R_{mh}} \tag{30}$$

$$\text{Rotor to Stator}: L_{rs} = \frac{d\underline{\Psi}^r_{hr}}{d\underline{i}^r_s} = \frac{N_r \cdot N_s}{R_{mh}} \tag{31}$$

The total flux linkage is the sum of the leakage flux and the main flux given as:

$$\begin{aligned}\text{Stator}: \underline{\Psi}^s_s &= (\underline{\Phi}_h + \underline{\Phi}_{\sigma s}) \cdot N_s = \underline{\Psi}^s_{hs} + \underline{\Psi}^s_{\sigma s} \\ &= \frac{N_s \cdot \underline{i}^s_s + N_s \cdot \underline{i}^s_r}{R_{mh}} \cdot N_s + \frac{N_s \cdot \underline{i}^s_s}{R_{m\sigma s}} \cdot N_s \\ &= L_{hs} \cdot \underline{i}^s_s + L_m \cdot \underline{i}^r_s + L_{\sigma s} \cdot \underline{i}^s_s \\ &= (L_{hs} + L_{\sigma s}) \cdot \underline{i}^s_s + L_m \cdot \underline{i}^r_s \\ &= L_s \cdot \underline{i}^s_s + L_m \cdot \underline{i}^r_s\end{aligned} \tag{32}$$

$$\begin{aligned}\text{Rotor}: \underline{\Psi}^r_r &= (\underline{\Phi}_h + \underline{\Phi}_{\sigma r}) \cdot N_r = \underline{\Psi}^r_{hr} + \underline{\Psi}^r_{\sigma r} \\ &= \frac{N_r \cdot \underline{i}^r_r + N_r \cdot \underline{i}^r_r}{R_{mh}} \cdot N_r + \frac{N_r \cdot \underline{i}^r_r}{R_{m\sigma r}} \cdot N_r \\ &= L_{hr} \cdot \underline{i}^r_r + L_m \cdot \underline{i}^r_r + L_{\sigma r} \cdot \underline{i}^r_r \\ &= (L_{hr} + L_{\sigma r}) \cdot \underline{i}^r_r + L_m \cdot \underline{i}^r_r \\ &= L_r \cdot \underline{i}^r_r + L_m \cdot \underline{i}^s_r\end{aligned} \tag{33}$$

### F. Torque

The law of conservation of energy leads to the equations of mechanical torque:

$$\underline{T} = \frac{3}{2} \cdot p \cdot (\underline{\Psi} \times \underline{i}) \tag{34}$$

where the factor $3/2$ comes from the scaling of the current space vector introduced earlier. The torque is given in the $(\alpha, \beta)$ coordinate system by the cross product of the corresponding stator flux linkage and the stator current:

$$T_e = \frac{3}{2} \cdot p \cdot (\underline{\Psi}^s_s \times \underline{i}^s_s) = \frac{3}{2} \cdot p \cdot (\underline{\Psi}^\alpha_s \cdot \underline{i}^\beta_s - \underline{\Psi}^\beta_s \cdot \underline{i}^\alpha_s) \tag{35}$$

### G. System Equations

The equations for the model of an AC machine are summarized below using (8),(9),(32),(33), and (35). This system of equations is generally employed for the analysis of an Induction Machine (IM) [29] and can also be used for a Permanent Magnet Synchronous machine (PMSM), but with a slight modification.

$$\underline{u}^s_s = R_s \cdot \underline{i}^s_s + \frac{d\underline{\Psi}^s_s}{dt} \tag{36a}$$

$$\underline{\Psi}^s_s = L_s \cdot \underline{i}^s_s + L_m \cdot \underline{i}^s_r \tag{36b}$$

$$\underline{u}^r_r = R_r \cdot \underline{i}^r_r + \frac{d\underline{\Psi}^r_r}{dt} \tag{36c}$$

$$\underline{\Psi}^r_r = L_r \cdot \underline{i}^r_r + L_m \cdot \underline{i}^r_s \tag{36d}$$

$$T_e = \frac{3}{2} \cdot p \cdot (\underline{\Psi}^s_s \times \underline{i}^s_s) \tag{36e}$$

$$J_m \frac{d\omega_m}{dt} = T_e - T_L - B \cdot \omega_m \tag{36f}$$

## III. Control methods for an Induction Machine

Unlike the DC machine, which is very sensitive to commutator failures, the IM has the advantage of a robust structure and low maintenance and therefore has been very popular for the realization of drive systems. Though R. H. Park [30] introduced rotating reference frames already in 1929, it took a long time to develop the idea of field-oriented control (FOC) that is based on the fundamental insight that the torque is proportional to the cross product of stator current and flux. The resulting decoupled control of torque and field excitation is then quite similar to DC motor control. In this section both the control schemes are discussed in detail.

### A. Field Oriented Control (FOC)

As discussed earlier the building block for FOC was the concept of Indirect FOC presented by Hasse in 1968 [15], [16]. However in 1971, Direct FOC (DFOC) was developed by Blaschke [17].

In the concept of Indirect FOC (IFOC), flux orientation is realized only by means of feed-forward control, typically by a calculation of the slip frequency from the reference values. This approach is simple and well performing for the speed and position control even at low speeds. However, the major drawback is, that the orientation of the control is very sensitive to the rotor resistance, which affects the robustness of the control. To overcome this problem the rotor resistance has to be estimated online [31], [32]. On the contrary, Direct FOC (DFOC) employs flux observers to calculate the flux orientation. The original approach of Blaschke [17] included flux measurement coils to accomplish the flux orientation.

Essentially for FOC the stator current space vector is decomposed into an flux forming and an torque-forming component by an appropriate coordinate transformation. Each component then is controlled individually by a linear PID (Proportional-Integral-Derivative) controller. For our analysis a squirrel cage IM is considered.

*1) Rotor Flux Oriented Coordinate System:* As demonstrated in previous sections, Park transformation ($\mathcal{T}_\mathcal{P}(\varphi_K)$) can be used to transform a space vector from the stator coordinates to the rotor coordinate system. For analysis of FOC the reference system is linked to the rotor flux axis rotating at synchronous speed. The advantage of using this reference frame is that all the quantities are constant in steady state, so it simplifies the fundamental wave model for control purposes. Since the *d*-axis is chosen along the rotor flux axis, it implies that the rotor flux is entirely along this axis i.e. $\Psi_r^d = \|\Psi_r\|$ and hence $\Psi_r^q = 0$. Therefore the rotor flux space vector in the rotated frame (Fig. 5) can be written as:

$$\underline{\Psi}_r = \begin{bmatrix} \Psi_r^d \\ \Psi_r^q \end{bmatrix} = \begin{bmatrix} \|\Psi_r\| \\ 0 \end{bmatrix} \tag{37}$$

Here $\varphi_K$ is the angle of the rotor flux space vector ($\Psi_r^s$) in stator coordinates (see Fig. 5). For this reason the defined $(d, q)$-coordinate system is called *rotor flux oriented* or commonly *field oriented.*

*2) Model of the Induction Machine in the d,q frame:* The mathematical model of the machine in the field oriented control system is formulated using the system of equations (36). The $(d, q)$-coordinate system is generalized using index *k*.

$$\underline{u}_s^k = R_s \cdot \underline{i}_s^k + \frac{d\underline{\Psi}_s^k}{dt} + j\omega_k \underline{\Psi}_s^k \text{ with } \omega_k = \dot{\varphi}_k \tag{38a}$$

$$\underline{\Psi}_s^k = L_s \cdot \underline{i}_s^k + L_m \cdot \underline{i}_r^k \tag{38b}$$

$$0 = R_r \cdot \underline{i}_r^k + \frac{d\underline{\Psi}_r^k}{dt} + j(\omega_k - \omega)\underline{\Psi}_r^k \tag{38c}$$

$$\underline{\Psi}_r^k = L_r \cdot \underline{i}_r^k + L_m \cdot \underline{i}_s^k \tag{38d}$$

The electromagnetic torque can be written as:

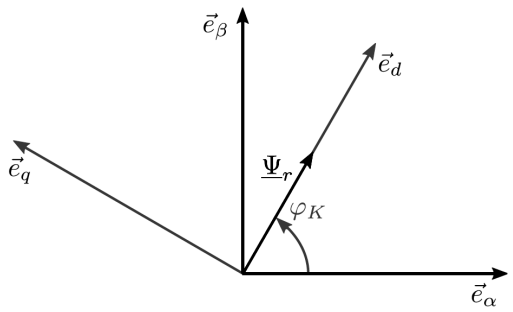


Fig. 5: Definition of the Rotor Flux Angle $\varphi_K$ used in the transformation $\mathcal{T}_\mathcal{P}(\varphi_K)$ [28].

$$\begin{aligned} T_e &= \frac{3}{2} \cdot p \cdot (\Psi_r^k \times i_r^k) = \frac{3}{2} \cdot p \cdot (\Psi_r^d \cdot i_r^q - \Psi_r^q \cdot i_r^d) \\ &= \frac{3}{2} \cdot p \cdot \Psi_r^d \cdot i_r^q = \frac{3}{2} \cdot p \cdot \|\Psi_r\| \cdot i_r^q \end{aligned} \tag{39}$$

Hence the torque is determined by the absolute value of the rotor flux space vector and the quadrature component of the rotor current ($i_r^q$). In a squirrel cage IM rotor currents cannot be influenced directly therefore a relation between the torque, the direct axis flux component and the current vector $i_s^d$ is derived below.
Since $\Psi_r^q = 0 \Rightarrow \dot{\Psi}_r^q = 0$, from (38d) we can write:

$$\begin{aligned} \Psi_r^q = 0 &= L_r \cdot i_r^q + L_m \cdot i_s^q \\ \Rightarrow\ i_r^q &= -\frac{L_m}{L_r} i_s^q \end{aligned} \tag{40}$$

From (38c) and (40) we can write the rotor voltage and the flux linkage equations as:

$$\begin{aligned} 0 &= R_r \cdot i_r^d + \frac{d\Psi_r^d}{dt} = \frac{R_r}{L_r}(\Psi_r^d - L_m \cdot i_s^d) + \frac{d\Psi_r^d}{dt} \\ \Rightarrow\ & \mathcal{T}_r \frac{d\Psi_r^d}{dt} + \Psi_r^d = L_m \cdot i_s^d \end{aligned} \tag{41}$$

Here $\mathcal{T}_r = L_r/R_r$ is the *rotor time constant*. Rearranging the above equation results in:

$$\Psi_r^d(s) = \frac{L_m}{1 + \mathcal{T}_r s}\, i_s^d(s) \tag{42}$$

From (42) one can suggest, that the absolute value of the rotor flux $\|\Psi_r\|$ can be manipulated by the direct axis component of the stator current, $i_s^d$, with the time constant $\mathcal{T}_r$. Hence we call $i_s^d$ as the *flux related* current component.

The torque equation from (39) and (40) can be written as:

$$T_e = \frac{3}{2} \cdot p \cdot \|\Psi_r\| \cdot i_r^q = \frac{3L_m}{2L_r} \cdot p \cdot \|\Psi_r\| \cdot i_s^q \tag{43}$$

If the value of rotor flux is maintained at a constant value, the torque can be controlled by the quadrature component of the stator current, $i_s^q$, without any time delay. Hence we call $i_s^q$ as the *torque related* current component.

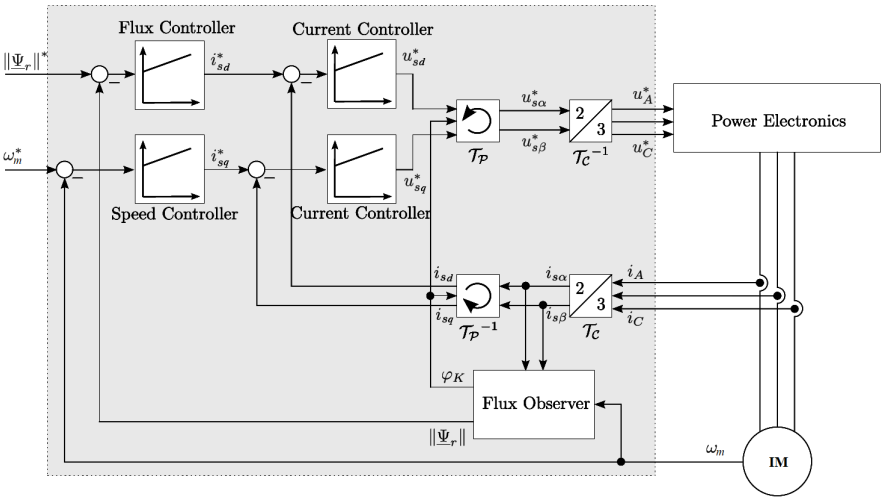


Fig. 6: Schematic representation of the Direct Field Oriented Control (DFOC) [28].

*3) Calculation of the Rotor Flux Vector:* Generally the flux linkage on the rotor side cannot be measured directly as it requires sophisticated equipment. Hence the rotor flux vector must be calculated from the measurable parameters like stator currents, stator voltages and rotational speed. To calculate the relation between the rotor flux vector and stator current vector we can derive a relation using (38c) and (38d). The relation can be written as:

$$\frac{d\underline{\Psi}_r^s}{dt} = -\frac{R_r}{L_r}(\underline{\Psi}_r^s - L_m \cdot \underline{i}_s^s) + j\omega \cdot \underline{\Psi}_r^s \tag{44}$$

This equation allows the calculation of rotor flux vector using stator currents and rotational speed $\omega$, however, the knowledge of the machine parameters $R_r, L_r$ and $L_m$ is a priori. These can be determined by the *No-Load* and *Blocked-Rotor* tests.

This approach requires the use of speed sensors or resolvers to measure the rotational speed of the machine or calculate the orientation of the rotor shaft. This type of FOC is famous as Direct FOC (DFOC). Fig. 6 gives a schematic view of the Direct FOC (DFOC). It must be noted that all of the cascaded controller blocks are linear PI based controllers. Additionally it is necessary to calculate flux using the flux observer, as rotor flux orientation $\varphi_k$ is essential for Park transform.

The FOC approach presented by Hasse in 1968 [15], [16], known as Indirect FOC takes a different approach. It uses the concept of slip speed $\omega_{slip}$ where the rotor flux orientation $\varphi_K$, required for coordinate transformation, is generated from the rotor speed $\omega_m$ and the slip speed $\omega_{slip}$:

$$\varphi_K = \int (\omega_e + \omega_{slip}) \cdot dt = \int (p \cdot \omega_m + \omega_{slip}) \cdot dt \tag{45}$$

The latter is calculated from the stator reference current $i_{sq}^*$ and the motor parameters:

$$\omega_{slip} = \frac{L_m R_r}{\Psi_r^d L_r} i_{sq}^* = \frac{L_m}{\Psi_r^d \mathcal{T}_r} i_{sq}^* \tag{46}$$

Fig. 7 depicts the basic structure of the Indirect FOC whereby the slip speed approach is used. The reference currents $i_{sd}^*$ and $i_{sq}^*$ are converted to the reference voltages in the $\alpha, \beta$-reference frame. These voltage values are then used to calculate the inverter gating signals $S_a, S_b, S_c$.

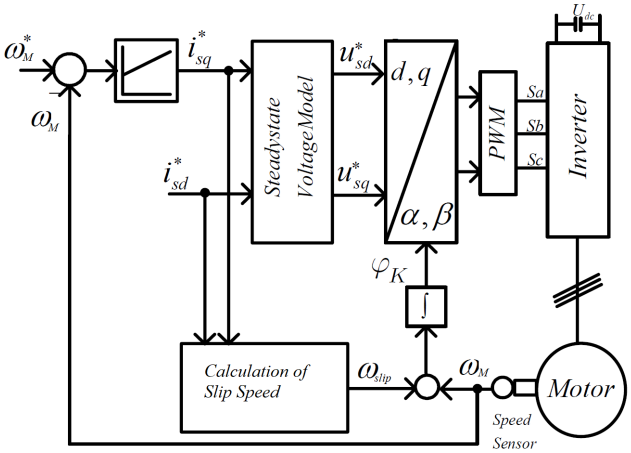


Fig. 7: Schematic representation of Indirect Field Oriented Control [33].

### B. Direct Torque Control (DTC)

Newer control methods were explored in the 1980s to overcome the complexity of the coordinate transformation where knowledge of the rotor orientation is necessary and hence the machine parameters. The machine parameters can be strongly dependent on the operating conditions, for example the stator or rotor resistances are influenced by temperature. If the parameters of the flux estimator do not match with the actual values, an estimation error occurs. This can have negative effects on the control accuracy. For this reason the field oriented control is not robust against parameter variations [28].

Development of advanced control strategies for PWM inverter fed Induction machine drives allowed the design of

control techniques without the need of coordinate transformation. *Direct Torque Control* is a consequence of the quest to avoid coordinate transformation and design a control strategy, independent of the machine parameters. Unlike FOC, flux and torque can be directly controlled by selecting appropriate inverter switching states [34]. Coupled with a better dynamic performance and simpler control strategy, DTC offers a very good alternative to FOC.

*1) Model of IM in Stationary Reference frame:* The mathematical model of the machine for DTC is again formulated using the system of equations (36). By applying Clarke transformation the system of equations can be referred to the stationary reference frame commonly known as $(\alpha, \beta)$-coordinate system.

$$\underline{u}_s^s = R_s \cdot \underline{i}_s^s + \frac{d\underline{\Psi}_s^s}{dt} \tag{47a}$$

$$\underline{\Psi}_s^s = L_s \cdot \underline{i}_s^s + L_m \cdot \underline{i}_r^s \tag{47b}$$

$$0 = R_r \cdot \underline{i}_r^s + \frac{d\underline{\Psi}_r^s}{dt} - j\omega\underline{\Psi}_r^s \tag{47c}$$

$$\underline{\Psi}_r^s = L_r \cdot \underline{i}_r^s + L_m \cdot \underline{i}_r^s \tag{47d}$$

$$T_e = \frac{3}{2} \cdot p \cdot (\underline{\Psi}_s^s \times \underline{i}_s^s) = \frac{3}{2} \cdot p \cdot (\underline{\Psi}_s^\alpha \cdot \underline{i}_s^\beta - \underline{\Psi}_s^\beta \cdot \underline{i}_s^\alpha) \tag{47e}$$

$$J_m \frac{d\omega_m}{dt} = T_e - T_L \tag{47f}$$

*2) Principle of Direct Torque Control:* In FOC the inverter firing signals $S_a, S_b, S_c$ are generated using a modulator. In practice, however, the converter can also be used without a modulator. DTC takes advantage of this possibility. In total the possible switching combinations for a 2 level inverter are $2^3 = 8$. The $(\alpha, \beta)$ plane is divided into six $60°$-wide vectors, designated $v_1$ through $v_6$ as illustrated in Fig 8. The space vectors $v_0, v_7$ short circuit the load and are called *zero space vectors* while the remaining ones are called *active space vectors*. A stator flux vector $(\underline{\Psi}_s^s)$ is said to be associated with the voltage vector $v_k$ when it passes through sector k. For example, the stator flux vector becomes associated with $v_2$ when passing sector 2.

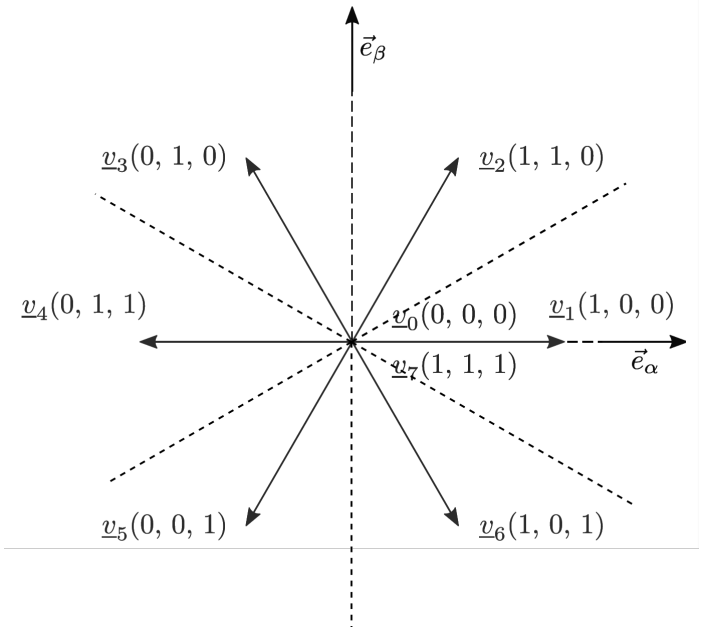


Fig. 8: Space vectors of the inverter output voltage and sectors.

*3) Approach:* With the background of the space vectors let us now consider the stator voltage equation (47a):

$$\underline{v}_k = \underline{u}_s^s = R_s \cdot \underline{i}_s^s + \frac{d\underline{\Psi}_s^s}{dt}, k \in \{0 \cdots 7\} \tag{48}$$

Suppose at time $t_0$ the converter switches from the voltage space vector $v_k$ to $v_l$ $(l \in \{0 \cdots 7\}, l \neq k)$, within the time interval $[t_0, t_0 + T_s]$. Since the switching time $T_s$ is very small as compared to the stator time constant $T_{\sigma s} = L_{\sigma s}/R_s$ the influence of the ohmic voltage drop in (48) can be neglected [28]. Hence we can write:

$$\underline{v}_l = \underline{u}_s^s \approx \frac{\Delta\underline{\Psi}_s^s}{T_s}, l \in \{0 \cdots 7\} \tag{49}$$

As illustrated in Fig. 9, application of voltage space vector $\underline{v}_l$ during the time interval $T_s$ leads to the following variation in the stator flux linkage:

$$\Delta\underline{\Psi}_s^s \approx T_s \cdot \underline{v}_l \tag{50}$$

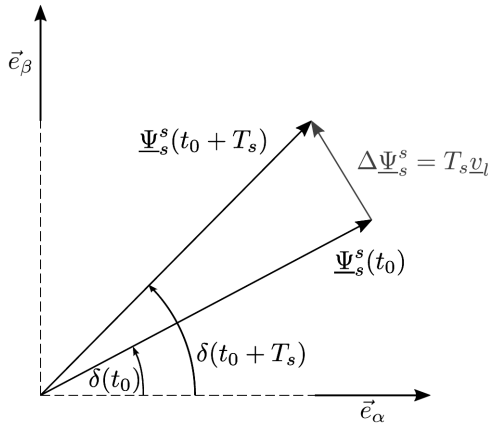


Fig. 9: Effect of vector $\underline{v}_l$ on $\underline{\Psi}_s^s$ [28].

Hence we can conclude that the trajectory of the space vector $\underline{\Psi}_s^s$ in the $(\alpha, \beta)$-plane can be determined by the application of a sequence of voltage space vectors [28]. In order to exploit this property let us derive a relation for the generated torque. Using (47b) and (47d) we can express the stator current as a function of $\underline{\Psi}_s^s$ and $\underline{\Psi}_r^s$, given as:

$$\underline{i}_s^s = \frac{1}{\sigma L_s}\left(\underline{\Psi}_s^s - \frac{L_m}{L_r}\underline{\Psi}_r^s\right) \text{ with } \sigma = 1 - \frac{L_m^2}{L_s L_r} \tag{51}$$

Substituting (51) into the torque equation (47e) we can write:

$$\begin{aligned} T_e &= \frac{3}{2\sigma L_s} \cdot p \cdot (\underline{\Psi}_s^s \times \left(\underline{\Psi}_s^s - \frac{L_m}{L_r}\underline{\Psi}_r^s\right)) \\ &= \frac{3pL_m}{2\sigma L_s L_r} \|\underline{\Psi}_s^s\| \cdot \|\underline{\Psi}_s^r\| \sin(\delta - \varphi) \end{aligned} \tag{52}$$

where $\delta$ and $\varphi$ are the angles of the stator and rotor flux vectors respectively, in the stationary reference frame. From (52) it can be inferred that torque can be determined by the absolute values of stator and rotor flux vectors and their relative angle.

Generally the rotor time constant $T_r = L_r/R_r$ is comparatively very large than the stator time constant $T_{\sigma s} = L_{\sigma s}/R_s$. $\underline{\Psi}_s^r$ can be assumed to be constant during the time interval $T_s$ and hence torque is essentially dependent only on the stator quantities.

*4) Formulation of the Control Concept:* As depicted in Fig. 8, by using the active space vectors of the converter the stator flux can be influenced in various ways within the time interval $T_s$. Regardless of the flux position, three of these voltage vectors lead to an increase in the magnitude of flux, while others decrease it. Furthermore, three of the space vectors lead to an anticlockwise rotation and hence increase the relative angle while the others tend to decrease the angle due to clockwise rotation. In order to control the

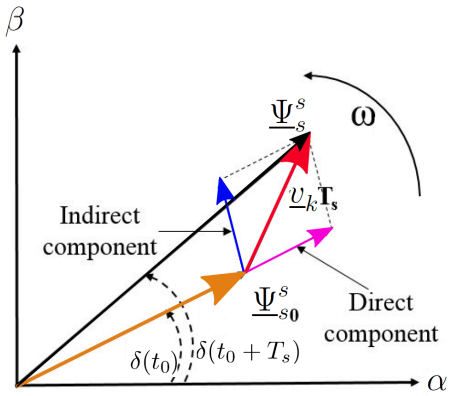


Fig. 10: Direct and indirect components of stator flux produced by voltage vectors.

stator flux and torque independently, it must be ensured that the magnitude of flux is controlled only by the application of appropriate voltage vectors whereas torque can be increased or decreased by changing the relative angle $(\delta - \varphi)$ within the interval $[-\pi/2; \pi/2]$. As shown in Fig. 10 the direct component of the voltage vector only contributes to the change in the magnitude of the stator flux vector while the indirect component is responsible for change in torque, as it changes the angle $\delta$.

Fig. 11 further illustrates the contribution of voltage vectors for flux and torque control. $\underline{\Psi}_s^s(t_0)$ is the initial flux vector. The magnitude of the flux can be increased by using vectors $v_2$ and $v_6$ since both the vectors have positive direct component. $v_3$ and $v_5$ can be used to decrease the flux magnitude. Moreover, both $v_2$ and $v_3$ voltage vectors have indirect components and contribute to an increase in torque where as $v_5$ and $v_6$ can be used to decrease the torque. Hence, $v_2$ can be used to increase both flux magnitude and torque angle. Similarly, voltage vector $v_5$ can be used to decrease both stator flux and torque [35], [36]. The relation between the voltage space vectors and their effects on the flux and torque within the respective sector

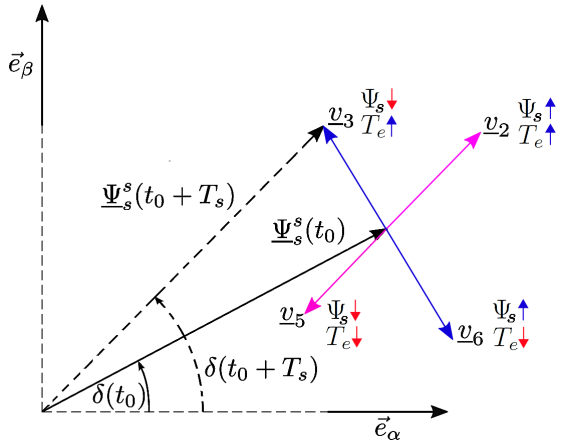


Fig. 11: Stator Flux $\Psi_s$ and Torque $T_e$ control using voltage vectors.

is summarized in a look up table (Table 2). The decision if the flux amount or the torque shall be increased respectively decreased, is taken by individual hysteresis controllers. The controllers are implemented in *discrete time* and work with the sampling time $T_s$.

The output value $h_{\underline{\Psi}_s}$ of the flux controller is determined by the control error $e_{\underline{\Psi}_s}$ sampled at the time instant $t_0 = nT_s$. Consequently a similar relation between the controller error $e_T$ and controller output $h_T$ of the torque controller also holds true. Fig. 12 [28] illustrates the operating scheme of the two hysteresis controllers.

Table II: Look up table for DTC [37].

| $h_{\underline{\Psi}_s}$ | $h_T$ | $S_1$ | $S_2$ | $S_3$ | $S_4$ | $S_5$ | $S_6$ |
|---|---|---|---|---|---|---|---|
| 1 | 1 | $V_2$ | $V_3$ | $V_4$ | $V_5$ | $V_6$ | $V_1$ |
| 1 | 0 | $V_0$ | $V_7$ | $V_0$ | $V_7$ | $V_0$ | $V_7$ |
| 1 | -1 | $V_6$ | $V_1$ | $V_2$ | $V_3$ | $V_4$ | $V_5$ |
| -1 | 1 | $V_3$ | $V_4$ | $V_5$ | $V_6$ | $V_1$ | $V_2$ |
| -1 | 0 | $V_7$ | $V_0$ | $V_7$ | $V_0$ | $V_7$ | $V_0$ |
| -1 | -1 | $V_5$ | $V_6$ | $V_1$ | $V_2$ | $V_3$ | $V_4$ |

The output of the torque controller can take the values -1, 0 and 1. The flux controller can only take the values -1 and 1. If the controller outputs the value -1, the corresponding control variable has to be decreased whereas, if the controller output is 1, the control variable should be increased. However for the torque controller if the output is 0, control variable shall remain constant.

*5) Summary of DTC Control:* From the above discussion control structure for the direct torque control can be derived. The control scheme with two hysteresis controllers and subsystems for flux estimator, torque estimator and the lookup table is shown in Fig. 13. Due to the switching behaviour of the hysteresis controllers, torque remains within a defined tolerance band, switching at a varied frequency between the two limits. This type of control is commonly known as *bang-bang control*. Additionally, the stator flux vector traces a zigzag shaped pattern around its setpoint in the $(\alpha, \beta)$-plane (Fig. 14).

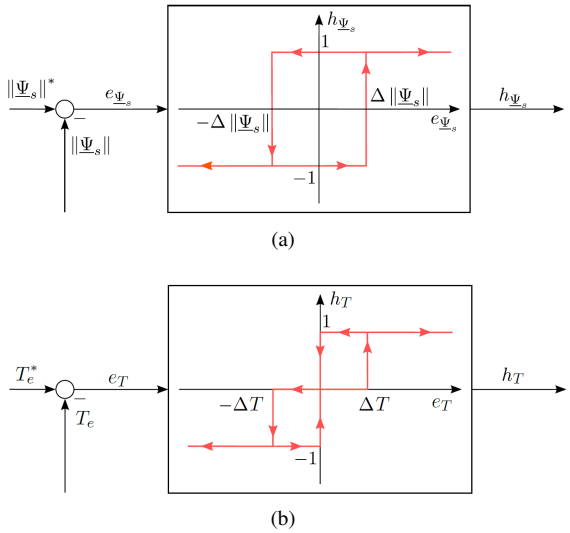


Fig. 12: Operating scheme of the hysteresis controllers [28].

## IV. Comparison of FOC and DTC for an Induction Machine

Both FOC and DTC schemes aim at controlling separately the motor torque and flux over a wide speed range. In this section first the two schemes are compared briefly and then the operating performance is evaluated.

Table III: Comparative issues in theory [38].

| | **FOC** | **DTC** |
|---|---|---|
| Tuned Parameters | 6 | 4 |
| External Controller | PI | PI |
| Inner Controller | 2 PI | 2 Hysteresis |
| Flux Angle | Yes | Yes |
| Coordinate Transformation | Yes | No |
| PWM | Yes | No |

### A. Basic Characteristics

Here the basic control characteristics of FOC and DTC are studied and compared with a view to defining the nature of the control strategies and examining their influence on the drive performance and on the implementation complexity.

*1) Flux and Torque Control Mechanism:* FOC scheme uses a $(d-q)$ reference frame having the d-axis aligned with the rotor flux vector that rotates at the stator frequency. This particular situation allows the flux and torque to be separately controlled by the $(d-q)$ components of stator current. The decoupling between flux and torque control is achieved only if the rotor flux position is accurately known.

On the other hand, DTC scheme uses a stationary $(\alpha, \beta)$ reference frame having $\alpha$-axis aligned with stator A-axis. Torque and flux are controlled by the stator voltage space vector $\underline{v}_l$ defined in the same reference frame.

*2) Controllers:* For FOC linear controllers, based on PI regulators, are used to control the flux and speed while the torque is indirectly controlled. Response is highly dependent on the tuning of these controllers and the linear operation range. On the contrary, DTC employs two independent hysteresis controllers to select the appropriate stator voltage vectors in order to maintain the torque and flux within the upper and lower bounds. This enables direct control of the two control parameters. The response time of hysteresis controllers is optimal but switching frequency is variable.

*3) Estimated Variables:* The operation of both FOC and DTC depends on the system variables that are computed or estimated from the measured quantities. The accuracy of the estimated variables has a direct influence on the control performance [39].

In FOC the estimated variable is the rotor flux angle $\varphi_K$, which is necessary for the coordinate transformation. A slight error in the calculation of the angle $\varphi_K$ can lead to undesirable coupling between the $(d-q)$ axes and hence invalidate the FOC operation. During transients, the rotor flux position may change and perfect decoupling can be temporarily lost.

In DTC the estimated quantities are the stator and motor torque, which are required for feedback control. The accuracy of stator flux depends mostly on the estimation accuracy on the stator resistance $R_s$, hence can affect the behaviour of both flux and torque control loops.

### B. Static and Dynamic Performance

In this section the performance for the two control schemes using simulation results is discussed and further conclusions are drawn towards the end. Simulations were not carried out but the discussion is based on the results from various articles. Simulation graphs have been reproduced here to compare the performance and draw final conclusions. Essentially the operating conditions and variable sensing are assumed to be ideal.

In order to make a fair comparison between the performance of the two control schemes it should be ensured that average switching frequency is approximately the same [40]. In FOC the switching frequency is adjusted by the PWM period. DTC, however, has variable switching frequency due to the hysteresis blocks, which are dependent on the operating point. Essentially, amplitude of the hysteresis bands has to be adjusted in order to achieve a mean inverter switching frequency practically equal to that of FOC scheme.

*1) Steady-State Performance:* In [40] the steady state performance was evaluated based on the current ripple. The results obtained for FOC and DTC have been summarised in tables 3 and 4, respectively. The considered operating conditions are related to rotor speed values of 100%, 50%, and 10% of the rated value, and torque values of 100%, 50%, and 0% of the rated value. As can be inferred from the tables FOC is characterised by lower current ripple compared to DTC.

Table IV: Current ripple for FOC [40].

| Torque \ Speed | 1440 rpm | 720 rpm | 144 rpm |
|---|---|---|---|
| 26.5 Nm | 0.64 A | 0.93 | 0.58 A |
| 13.25 Nm | 0.64 A | 0.94 | 0.34 A |
| 0 Nm | 0.65 A | 0.93 | 0.34 A |

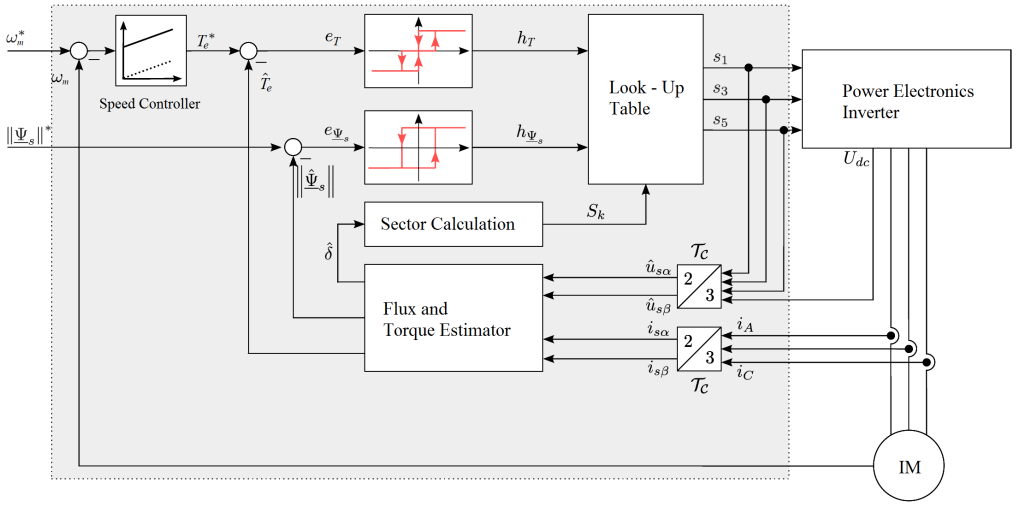


Fig. 13: Schematic representation of Direct Torque Control [28].

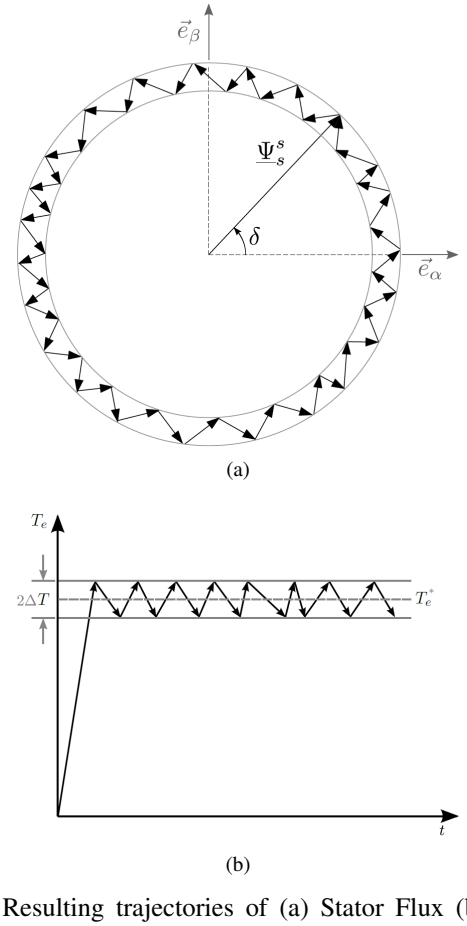

(a)

(b)

Fig. 14: Resulting trajectories of (a) Stator Flux (b) Torque [28].

Figs. 15 and 16 depict the torque, stator current, and stator current harmonic spectrum obtained for FOC and DTC respectively. Under the assumption of the same average inverter switching frequency, the amplitude of the torque ripple in DTC is slightly higher than that of FOC. Additionally it can be inferred from the harmonic spectrum of the stator currents, DTC has relatively larger variety of harmonics compared to FOC. Accordingly FOC generates a high frequency uniform noise, whereas DTC produces an irregular noise level, which is particularly maddening at low speed [40].

Table V: Current ripple for DTC [40].

| Torque \ Speed | 1440 rpm | 720 rpm | 144 rpm |
|---|---|---|---|
| 26.5 Nm | 1.10 A | 1.57 | 1.46 A |
| 13.25 Nm | 1.09 A | 1.56 | 1.27 A |
| 0 Nm | 1.18 A | 1.46 | 1.21 A |

*2) Dynamic Performance:* The transient performance of the two schemes is compared by analyzing a step response for torque at different rotor speeds. Fig. 17(a)–(c) illustrate the torque responses obtained using FOC scheme, at 1200, 600, and 100 rpm, respectively. Fig. 18(a)–(c) illustrate the same quantities obtained using DTC scheme. The results show that DTC has a better torque response in terms of the settling time and overshoot whereas FOC has a longer settling time. The difference in dynamic behaviour can be attributed to the use of PI regulators in FOC, which produce a delayed torque response in comparison to DTC, which exhibits a better dynamic response.

### C. Comparison of Parameter Sensitivity

As stated earlier, both FOC and DTC are based on estimated variables and their accuracy has direct influence on the control performance.

*1) Parameter Sensitivity of FOC:* Calculation of flux in FOC (42) is primarily dependent on stator current $i_s^d$ and the rotor time constant $\mathcal{T}_r = L_r/R_r$. The rotor resistance varies as a function of the temperature while the rotor inductance changes with flux level. An error in the estimation of $\mathcal{T}_r$, will deteriorate the control performance.

$u^2$

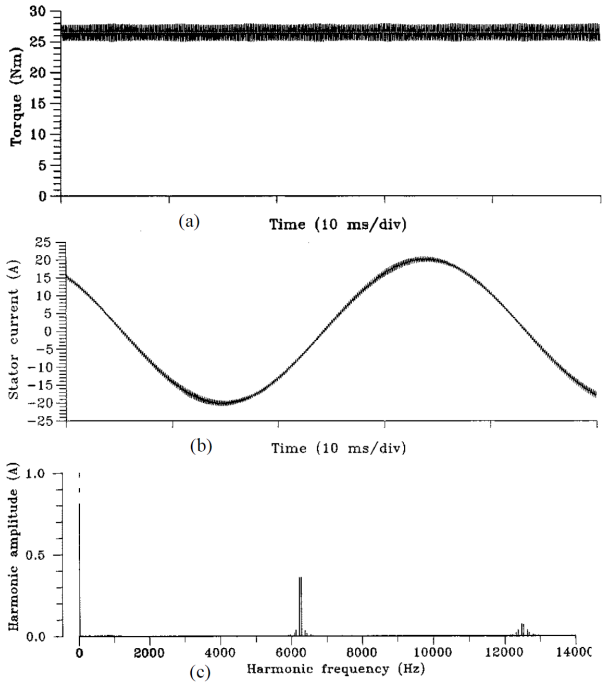


Fig. 15: Steady state (a) Torque, (b) Stator Current and (c) Stator current harmonic spectrum for FOC scheme [40].

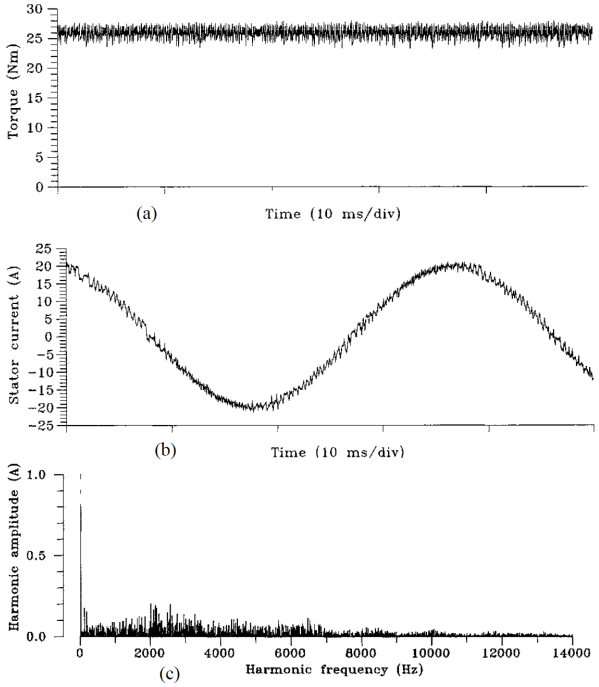


Fig. 16: Steady state (a) Torque, (b) Stator Current and (c) Stator current harmonic spectrum for DTC scheme [40].

To study the extent of estimation error in $R_r$ the authors in [39] observed the torque and flux responses by applying a step change in $R_r$ with motor in steady state operation. Fig. 19 shows the variation of rotor flux and torque for the cases where the estimated value of $R_r$ is suddenly changed to 75% and 125% of the actual value. In both situations the variation in parameters is significant and control performance deteriorates. The dependence of FOC operation on the rotor time constant can be minimized by using an improved flux observer [39].

*2) Parameter Sensitivity of DTC:* DTC operation is essentially based on the calculated value of stator flux which depends on the stator resistance $R_s$. Primarily at low speeds the value of $(v_s - R_s.i_s)$ is pretty small and a slight variation in the value of $R_s$ can produce inaccurate results, resulting in the deterioration of the control performance.

The extent of estimation error in $R_s$ is studied by applying a step change in $R_s$ with the motor running at 1 rad/s and the results obtained are presented in Fig. 20. As can be observed, the responses of flux and torque deviate from the reference indicating poor control performance. Low speed operation of DTC can be improved by using an improved stator flux estimation algorithm for this speed range [41].

### *D. Summary*

Table 6 presents a comparative summary of the results presented in the previous sections. DTC has an advantage over FOC in terms of dynamic flux control and implementation complexity.

## V. Control Methods for PMSM

Permanent magnet synchronous machines (PMSM) have found increasing application in the industrial drives domain primarily due to the high power density (compactness), high efficiency, ease of control, high torque-inertia ratio and better reliability. Since 1980s a considerable amount of research and development has been undertaken and PMSMs have shown increasing promise for industrial drive applications [42]–[44]. The PMSM has a stator which resembles the conventional synchronous machine (SM). However, the rotor excitation is supplied using permanent magnets. The main advantage when compared to the conventional SM is the elimination of the field coil, DC supply and slip rings; hence, lower losses and a less complex machine [14]. Since there is no provision for the control of excitation on the rotor side, control of a PMSM is done entirely through the stator excitation.

In principle, the construction of a permanent magnet synchronous machine does not differ from that of the BLDC, although distributed windings are more often used. However, unlike BLDC, sinusoidal excitation is used with PMSMs, which eliminates the torque ripple caused by the commutation. The PMSM has essentially two different configurations: surface mounted (Fig. 21) and interior (or buried) magnet (Fig. 22). The location of the magnets has a significant effect on the motor's mechanical and electrical characteristics, especially on the inductances of the machine. Particularly in case of the surface magnet construction the direct-axis inductance is very low, which has a substantial effect on the machine's overloading capability, and also on the field weakening characteristics. As the pull-out torque is inversely proportional to the

Table VI: Comparison of FOC and DTC w.r.t an IM [39].

| | **Field-Oriented Control** | **Direct Torque Control** |
|---|---|---|
| Frame of Reference | Synchronously rotating $(d-q)$ | Stationary $(\alpha, \beta)$ |
| Controlled variables | Torque $(T_e)$, Rotor Flux $(\Psi_r)$ | Torque $(T_e)$, Stator Flux $(\Psi_s)$ |
| Control parameters | Stator currents | Stator voltage space vector |
| Sensed variables | Rotor mechanical speed, Stator currents | Stator voltages, Stator currents |
| Estimated variables | Rotor flux position $(\varphi_k)$, Slip frequency $(\omega_{slip})$ | Torque, Stator flux |
| Controllers | Linear controllers for Stator currents | Hysteresis controllers for Torque and Stator flux |
| Torque Control | Indirectly controlled by stator currents, High dynamics, Torque ripple | Directly controlled, High dynamics, Controlled Torque ripple |
| Flux Control | Indirectly controlled by stator currents, Slow dynamics | Directly controlled, Fast dynamics |
| Parameter sensitivity | Sensitive to rotor time constant $(\mathcal{T}_r)$ | Sensitive to stator resistance $(R_s)$ |
| Implementation Complexity | High complexity, Coordinate transformation necessary | Medium complexity, No coordinate transformation |

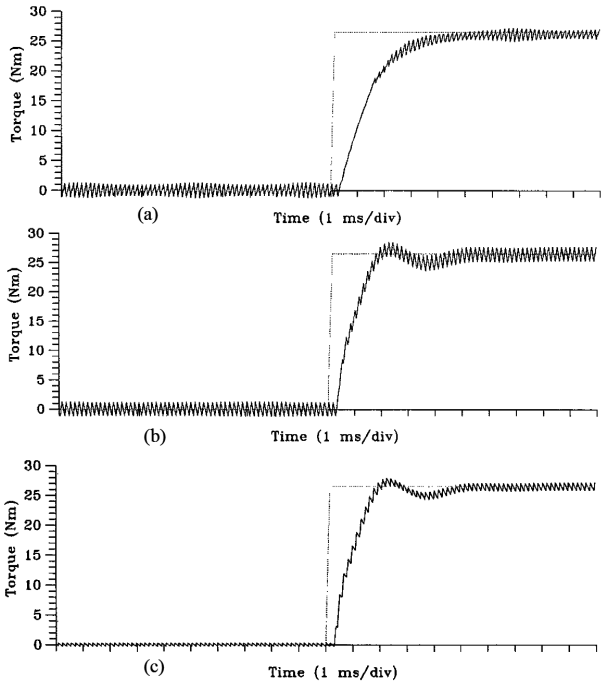


Fig. 17: Torque response at (a) 1200 rpm, (b) 600 rpm and (c) 100 rpm for FOC scheme [40].

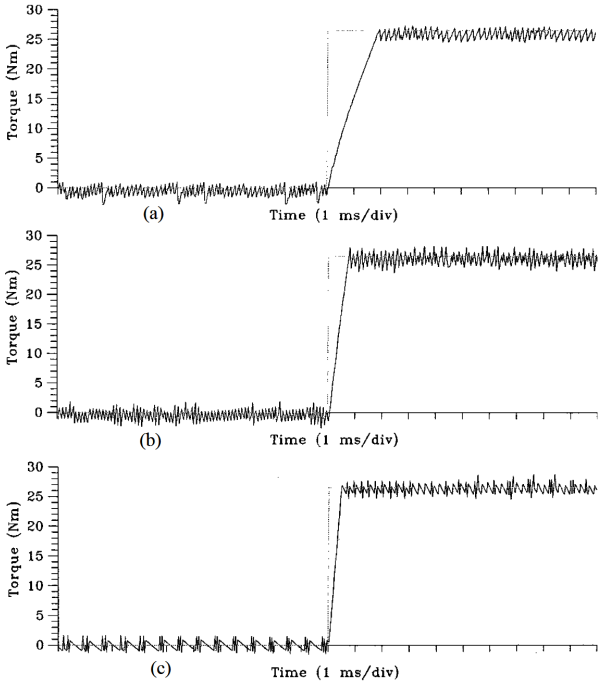


Fig. 18: Torque response at (a) 1200 rpm, (b) 600 rpm and (c) 100 rpm for DTC scheme [40].

d-axis inductance, the pull-out torque becomes very high. In contrast to this the direct-axis inductance of a machine having embedded magnets is higher. However the surface magnet construction is favourable in servo applications due to the lower inertia of the machine.

The buried magnet PMSMs are robust and thus permit higher operating speed. The effective airgap in this class of machines is low and therefore armature reaction effect is very dominant. This permits control of the machine in constant-torque region as well as in field-weakening constant-power region, upto such high speeds that the machine can be used for traction type applications [43]. Again, the saliency $(X_s^q > X_s^d)$ in this type of machine permits economical machine design because torque is contributed by both excitation and reluctance torques.

Since the introduction of new materials like neodymium-iron-boron (NdFeB) in 1983 PMSMs gained a lot of popularity and industrial application. The main advantages of PMSM are [45], [46]:

- Lower maintenance due to the absence of brushes and slip rings.
- Lower inertia and better dynamic performance.
- No rotor losses due to the absence of windings in the rotor, hence higher efficiency.
- Higher power/weight ratio.

The merits are counterbalanced by the higher cost and the variation of the PM properties due to temperature changes over the period of operation. PMSMs are currently employed

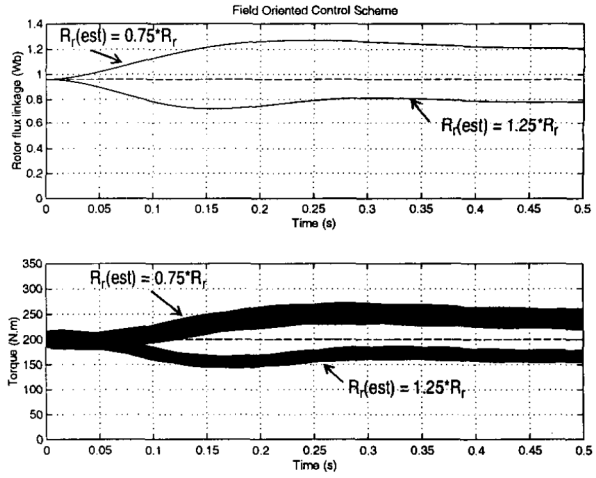


Fig. 19: Influence of estimated rotor resistance on performance of FOC [39].

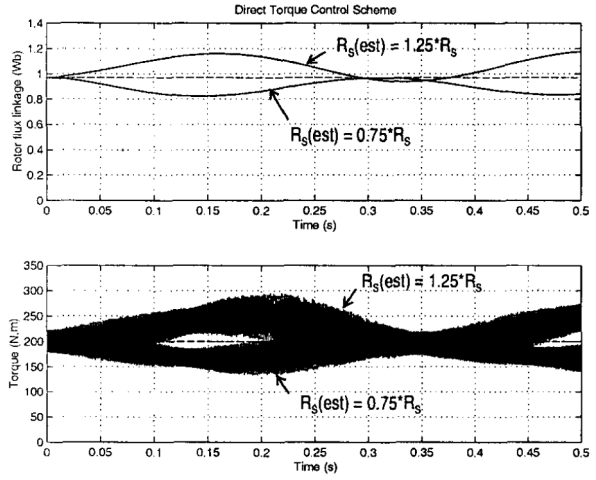


Fig. 20: Influence of estimated stator resistance on performance of DTC [39].

in applications where high acceleration and precise control is required such as robotics and machine tools.

### A. Model of PMSM

The analysis of a synchronous machine with permanent magnets can also be carried out using the fundamental wave model presented in (36). In PMSM the rotor windings are replaced by permanent magnets. Consequently the rotor flux is constant (denoted as $\Psi_{PM}$) and the rotor current $i_r^r$ is zero. Hence the system of equations (36) reduce to:

$$\underline{u}_s^s = R_s \cdot \underline{i}_s^s + \frac{d\underline{\Psi}_s^s}{dt} \tag{53a}$$

$$\underline{\Psi}_s^s = L_s \cdot \underline{i}_s^s + \underline{\Psi}_{PM}^s \tag{53b}$$

$$T_e = -\frac{3}{2} \cdot p \cdot (\underline{\Psi}_s^s \times \underline{i}_s^s) \tag{53c}$$

$$J_m \frac{d\omega_m}{dt} = T_e - T_L - B \cdot \omega_m \tag{53d}$$

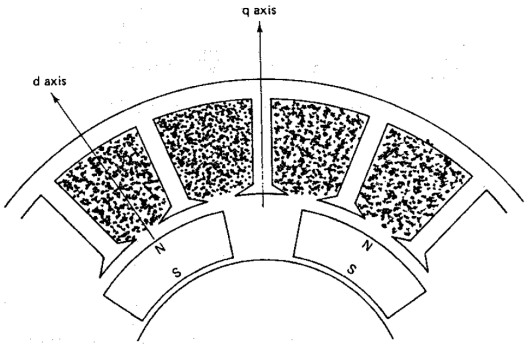


Fig. 21: Surface Mounted PMSM [14].

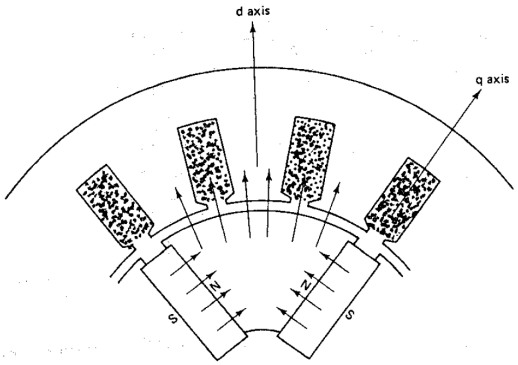


Fig. 22: Interior (or buried) PMSM [14].

### B. Field Oriented Control

Like the IM, FOC is applied to the PMSM to achieve decoupled control of torque and flux. The underlying principles for the application of FOC to a PMSM are the same as described in earlier sections. However, due to the permanent magnets on the rotor the generated rotor flux is constant and independent of the d-axis current $i_s^d$ (unlike the IM, from (42)). Hence the reference value for $i_s^d$ is set to zero, which in turn decreases the stator current and increases the efficiency of the drive. The torque equation (43) for the IM is modified for the PMSM as follows:

$$T_e = -\frac{3}{2} \cdot p \cdot \Psi_{PM} \cdot i_s^q \tag{54}$$

From (54) it is apparent that the electromagnetic torque is proportional to $i_s^q$. As indicated above, due to the constant nature of the rotor flux the d-axis component is set to zero, whereas the generated torque is linearly proportional to the q-axis component $i_s^q$ (essentially the major part of stator current), maximum torque per ampere (MTPA) can be achieved [47].

### C. Direct Torque Control

Since the analysis of DTC is carried in the stationary coordinates, $(\alpha, \beta)$-frame, the application remains more or less the same, as described in Section 3.2, with a slight modification of the rotor flux to a constant value $\Psi_{PM}$.

Table VII: Comparison of FOC and DTC w.r.t a PMSM [48].

| | **Field-Oriented Control** | **Direct Torque Control** |
|---|---|---|
| Dynamic response for torque | Slower | Faster |
| Steady-state behaviour for torque, stator flux and currents | Lower ripple and distortion | Higher ripple and distortion |
| Parameter sensitivity | Decoupling depends on $L_s^d, L_s^q, \Psi_{PM}$ | Sensitive to stator resistance $(R_s)$ |
| Controllers | Linear PI regulators for Stator currents | Hysteresis controllers for Torque and Stator flux |
| Switching Frequency | Constant | Variable |
| Implementation Complexity | High complexity, Coordinate transformation necessary | Medium complexity, No coordinate transformation |

### *D. Comparison*

A detailed comparison of the performance of FOC and DTC for a PMSM can be found in [47]–[49]. In essence, the responses of both the control schemes are similar for the IM (described in Section 4) and PMSM. A major difference, however, is that FOC is sensitive to rotor resistance variations in case of an IM whereas due to the use of permanent magnets in PMSM the sensitivity reduces. Due to this the dependency on rotor time constant decreases and hence dynamic performance improves. Overall it can be concluded that FOC has good steady state characteristics whereas DTC shows better dynamic performance.

Table VII presents a brief comparison of various factors with specific reference to PMSMs. Although the fundamental differences between FOC and DTC are independent of the type of machine used, specific parameters have been included in the Table VII.

## VI. Conclusion

In this paper, a comparison of the two vector control methods: FOC and DTC was carried out for an IM and a PMSM and an attempt, to compare the pros and cons of both the methods for the specific machine, was made. It is quite difficult to clearly state the superiority of one scheme over the other because of the balance of merits of the two schemes. Based on the discussion and the presented results, one can nevertheless say that the two control schemes provide, in their basic configuration, comparable performance regarding torque control. Summarizing, it can be said that both methods provide a good performance with quicker torque dynamics in case of DTC and better steady-state behaviour for FOC.

Additionally PMSMs have the advantage of compact and smaller drives for the same power rating. Both IMs and PMSMs are used in specific applications and have respectable market shares. It should, however, be noted that the lower inductance of the PMSM compared to an IM causes higher torque ripples with DTC and in order to reduce the ripple to an acceptable level, lower sampling times have to be employed.

In a nutshell, depending on the requirements of a particular application one control method can be more suitable than the other. With the use of advanced techniques both FOC and DTC can be improved to deliver better, improved, and comparable performance.

## References


[1] Dave, W., 2015. Field-Oriented Motor Control: Historical Foundations, accessed 28.12.17, (www.eetimes.com/author.asp?doc_id=1325757).

[2] Puranen, J., 2006. Induction motor versus permanent magnet synchronous motor in motion control applications: a comparative study. Doctoral Dissertation, Acta Universitatis Lappeenrantaensis.

[3] Wang, W., Cheng, M., Hua, W., Zhao, W., Ding, S. and Zhu, Y., 2010, October. An improved stator flux observation strategy for direct torque controlled induction machine drive system. In Electrical Machines and Systems (ICEMS), 2010 International Conference on (pp. 863-867). IEEE.

[4] Hussain, S. and Bazaz, M.A., 2015, March. Review of vector control strategies for three phase induction motor drive. In Recent Developments in Control, Automation and Power Engineering (RDCAPE), 2015 International Conference on (pp. 96-101). IEEE.

[5] Merzoug, M.S., Benalla, H. and Naceri, H., 2009, December. Speed estimation using extended filter Kalman for the direct torque controlled permanent magnet synchronous motor (PMSM). In Computer and Electrical Engineering, 2009. ICCEE'09. Second International Conference on (Vol. 2, pp. 122-127). IEEE.

[6] Wang, Y., Zhu, J.G. and Guo, Y.G., 2007, December. A survey of direct torque control schemes for permanent magnet synchronous motor drives. In Power Engineering Conference, 2007. AUPEC 2007. Australasian Universities (pp. 1-5). IEEE.

[7] Wang, Y. and Zhu, J., 2008, October. Modelling and implementation of an improved DSVM scheme for PMSM DTC. In Electrical Machines and Systems, 2008. ICEMS 2008. International Conference on (pp. 1042-1046). IEEE.

[8] Alam, S.M., 2016. Direct Torque Control of AC Machine Drives. Master Thesis, Southern Illinois University at Edwardsville.

[9] Kovács, K.P. and Rácz, I., 1959. Transiente vorgänge in Wechselstrommaschinen (Vol. 1). Verlag der ungarischen Akademie der Wissenschaften.

[10] Schonung, A., H. Stemmler, 1964. Static frequency changers with subharmonic control in conjunction with reversible variable-speed ac drives. Brown Boveri Review, 555.

[11] Zidani, F., Nait-Said, M.S., Abdessemed, R. and Benoudjit, A., 1998, August. Induction machine performances in scalar and field oriented control. In Power System Technology, 1998. Proceedings. POWERCON'98. 1998 International Conference on (Vol. 1, pp. 595-599). IEEE.

[12] Krein, P.T., Disilvestro, F., Kanellakopoulos, I. and Locker, J., 1993, June. Comparative analysis of scalar and vector control methods for induction motors. In Power Electronics Specialists Conference, 1993. PESC'93 Record., 24th Annual IEEE (pp. 1139-1145). IEEE.

[13] Dewan, S.B., Slemon, G.R. and Straughen, A., 1984. Power semiconductor drives. Wiley-Interscience.

[14] Sen, P.C., 1990. Electric motor drives and control-past, present, and future. IEEE Transactions on Industrial Electronics, 37(6), pp.562-575.

[15] Hasse, K., 1968, Zum dynamischen Verhalten der Asynchronmaschine bei Betrieb mit variabler Ständerfrequenz und Ständerspannung, ETZ-A Bd., 89, p.77.

[16] Hasse, K., 2001, November. Feldorientierte Regelung im Rückblick. In IEEE IAS/PELS/IES German Chapter Meeting, Braunschweig (Vol. 22).

[17] Blaschke, F., 1972, The principle of field orientation applied to the new trans-vector closed-loop control system for rotating field machines, Siemens-Review 39, pp. 217–220.

[18] Ho, E.Y. and Sen, P.C., 1988. Decoupling control of induction motor drives. IEEE Transactions on Industrial Electronics, 35(2), pp.253-262.
[19] Xu, X., De Doncker, R. and Novotny, D.W., 1988, April. A stator flux oriented induction machine drive. In Power Electronics Specialists Conference, 1988. PESC'88 Record., 19th Annual IEEE (pp. 870-876). IEEE.
[20] De Doncker, R.W. and Novotny, D.W., 1994. The universal field oriented controller. IEEE Transactions on Industry applications, 30(1), pp.92-100.
[21] Depenbrock M., 1988, Direct self-control (DSC) of inverter-fed induction machine. IEEE Transactions on Power Electronics, 3(4), pp. 420-429.
[22] Depenbrock, M., BBC Brown Boveri and Co Ltd, Germany, 1987. Direct self-control of the flux and rotary moment of a rotary-field machine. U.S. Patent 4,678,248.
[23] Takahashi, I. and Noguchi, T., 1986. A new quick-response and high-efficiency control strategy of an induction motor. IEEE Transactions on Industry applications, (5), pp.820-827.
[24] Baader, U., Depenbrock, M. and Gierse, G., 1992. Direct self control (DSC) of inverter-fed induction machine: A basis for speed control without speed measurement. IEEE transactions on industry applications, 28(3), pp.581-588.
[25] Jänecke, M., Kremer, R. and Steuerwald, G., 1989. Direct self control, a novel method of controlling asynchronous machines in traction applications. In Record of the EPE-Conference., pp. 75–81
[26] Habetler, T.G., Profumo, F., Pastorelli, M. and Tolbert, L.M., 1992. Direct torque control of induction machines using space vector modulation. IEEE Transactions on Industry Applications, 28(5), pp.1045-1053.
[27] Buja, G.S. and Kazmierkowski, M.P., 2004. Direct torque control of PWM inverter-fed AC motors-a survey. IEEE Transactions on industrial electronics, 51(4), pp.744-757.
[28] Manoharan, D., Sept. 2017. Practical Course on Simulation and Optimization of Mechatronic Drive Systems for MSPE. (www.eal.ei.tum.de/index.php?id=pcsomdsmspe00)
[29] Begh M.A.W. and Sharma B.B., 2017. Impact of Parametric Variations on Chaotic Behaviour of Indirect Field Controlled Induction Motor Drives. International Journal of Engineering Trends and Technology (IJETT), V54(1),41-47 December 2017. ISSN:2231-5381.
[30] Park, R.H., 1929. Two-reaction theory of synchronous machines generalized method of analysis-part I. Transactions of the American Institute of Electrical Engineers, 48(3), pp.716-727.
[31] Garces, L.J., 1980. Parameter adaption for the speed-controlled static ac drive with a squirrel-cage induction motor. IEEE Transactions on Industry Applications, (2), pp.173-178.
[32] Gabriel, R.,1982. Feldorientierte Regelung einer Asynchronmaschine mit einem Mikrorechner. Dissertation, TU Braunschweig.
[33] Bocker, J. and Mathapati, S., 2007, May. State of the art of induction motor control. In Electric Machines & Drives Conference, 2007. IEMDC'07. IEEE International (Vol. 2, pp. 1459-1464). IEEE.
[34] Bose, B.K., 2010. Power electronics and motor drives: advances and trends. Elsevier.
[35] Ozturk, S.B., 2008. Direct torque control of permanent magnet synchronous motors with non-sinusoidal back-EMF. Texas A&M University.
[36] Pai, D., Mangsuli, P.R. and Rao, N.J., 2000. Nonlinear observer based sensorless direct torque control of induction motor. In Power Electronics and Motion Control Conference, 2000. Proceedings. IPEMC 2000. The Third International (Vol. 1, pp. 440-445). IEEE.
[37] Arias Pujol, A., 2001. Improvements in direct torque control of induction motors. Dissertation, Universitat Politècnica de Catalunya.
[38] Wang, F., Zhang, Z., Mei, X., Rodríguez, J. and Kennel, R., 2018. Advanced Control Strategies of Induction Machine: Field Oriented Control, Direct Torque Control and Model Predictive Control. Energies, 11(1), p.120.
[39] Le-Huy, H., 1999. Comparison of field-oriented control and direct torque control for induction motor drives. In Industry Applications Conference, 1999. Thirty-Fourth IAS Annual Meeting. Conference Record of the 1999 IEEE (Vol. 2, pp. 1245-1252). IEEE.
[40] Casadei, D., Profumo, F., Serra, G. and Tani, A., 2002. FOC and DTC: two viable schemes for induction motors torque control. IEEE transactions on Power Electronics, 17(5), pp.779-787.
[41] Buja, G., Casadei, D. and Serra, G., 1997, November. DTC-based strategies for induction motor drives. In Industrial Electronics, Control and Instrumentation, 1997. IECON 97. 23rd International Conference on (Vol. 4, pp. 1506-1516). IEEE.
[42] Weh, H., Mosebach, H. and May, H., 1984. Design concepts and force generation in inverter-fed synchronous machines with permanent magnet excitation. IEEE Transactions on Magnetics, 20(5), pp.1756-1761.
[43] Bose, B.K. and Szczesny, P.M., 1988. A microcomputer-based control and simulation of an advanced IPM synchronous machine drive system for electric vehicle propulsion. IEEE transactions on industrial electronics, 35(4), pp.547-559.
[44] Rekioua, T., Tabar, F.M. and Le Doeuff, R., 1990, July. A new approach for the field-oriented control of brushless, synchronous, permanent magnet machines. In Power Electronics and Variable-Speed Drives, 1990. Fourth International Conference on (Conf. Publ. No. 324) (pp. 46-50). IET.
[45] Vas, P., 1998. Sensorless vector and direct torque control. Oxford Univ. Press.
[46] Fitzgerald, A.E., Kingsley, C., Umans, S.D. and James, B., 2003. Electric machinery (Vol. 5). New York: McGraw-Hill.
[47] Shyu, K.K., Lai, C.K., Tsai, Y.W. and Yang, D.I., 2002. A newly robust controller design for the position control of permanent-magnet synchronous motor. IEEE Transactions on Industrial Electronics, 49(3), pp.558-565.
[48] del Toro Garcia, X., Zigmund, B., Terlizzi, A.A., Pavlanin, R. and Salvatore, L., 2006. Comparison between FOC and DTC strategies for permanent magnet synchronous motors. Advances in Electrical and Electronic Engineering, 5(1-2), p.76.
[49] Kronberg, A., 2012. Design and simulation of field oriented control and direct torque control for a permanent magnet synchronous motor with positive saliency. Master Thesis, Uppsala University.



View publication stats